R_s being the sun radius and L the astronautical unit (see Fig. 1). Combining Eqs. (3–5), we get

$$\cos^2\phi \cos^2\gamma = \left\{\frac{1 + e\cos(\phi - \alpha)}{a(1 - e^2)} \times \left[R_e \sin\sigma + \cos\sigma\left(\left[\frac{a(1 - e^2)}{1 + \cos(\phi - \alpha)}\right] - R_e^2\right)^{1/2}\right]\right\}^2 \quad (7)$$

where the satellite orbit, in plane polar coordinates, was assumed to be given (neglecting perturbation effects) by

$$r = \frac{a(1 - e^2)}{1 + e\cos(\phi - \alpha)} \quad (8)$$

a being the semimajor axis of the orbit.

Subscript 1 was omitted in (7) and (8), since a similar expression to (7) can be obtained by repeating the development in Fig. 3 for r_2, the radius vector at the point where the satellite leaves the umbra. In that case, Eq. (7) would be given in terms of ϕ_2 instead of ϕ_1.

There are four distinct roots (for ϕ) to Eq. (7). Since the umbra is displaced 180° from the solar vector projection (see Fig. 2), the only pertinent roots are those in the second and third quadrant. These roots correspond to umbra entry and exit, respectively. (Recall that ϕ is measured from the solar vector projection.) For a given α, γ and orbital elements e and a, we can determine ϕ_1 and ϕ_2 from Eq. (7) by the following criteria:

$$\phi = \phi_1 \quad \text{if} \quad \pi > \phi > \pi/2 \quad (9)$$

$$\phi = \phi_2 \quad \text{if} \quad 3\pi/2 > \phi > \pi \quad (10)$$

The umbra eclipse factor ϵ_u can then be found from Eq. (2).

2. *Penumbra eclipse factor*

The analysis for the penumbra eclipse factor is similar to that of the umbra eclipse factor. The penumbra eclipse factor is defined as the ratio of the time a satellite is occulted by the earth penumbra to the time of a complete satellite orbit and is given by

$$\epsilon_p = \epsilon_u(\phi'_1, \phi'_2) - \epsilon_u(\phi_1, \phi_2) \quad (11)$$

where $\epsilon_u(\phi_1, \phi_2)$ is obtained from Eq. (2) evaluated at ϕ_1 and ϕ_2, and $\epsilon_u(\phi_1', \phi_2')$ is obtained from Eq. (2) evaluated at ϕ_1' and ϕ_2' (see Fig. 2). The angles ϕ_1' and ϕ_2' are obtained from Eq. (7) in the same manner as ϕ_1 and ϕ_2, except that σ is replaced by $-\sigma'$ where σ' is the penumbra half-cone angle (see Fig. 1) and is given by

$$\sigma' = \sin^{-1}\left[\frac{R_s}{L}\left(1 + \frac{R_e}{R_s}\right)\right] \quad (12)$$

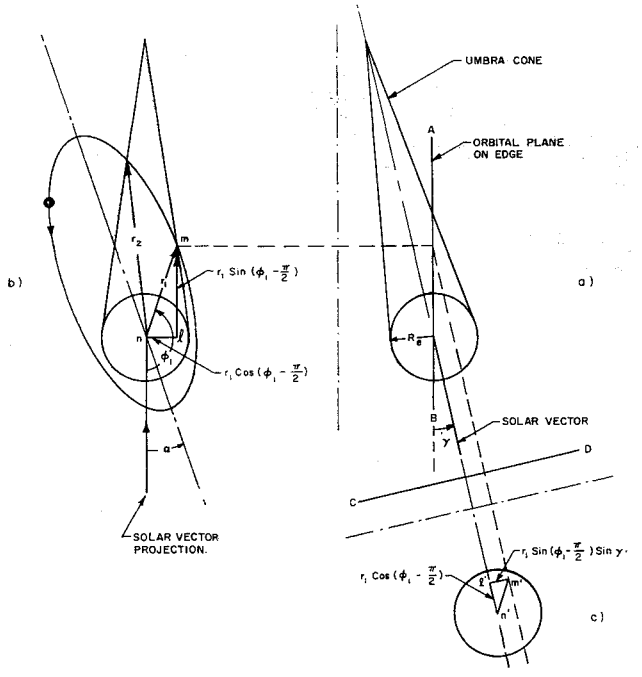

Fig. 3 Geometry for the determination of umbra eclipse factor.

E. Computing Program

The method described previously for calculating umbra and penumbra eclipse factors lends itself to a straightforward hand calculation. The only difficult step is the solving of Eq. (7), which is transcendental and requires assumptions and iterations. To avoid this difficulty, the analysis was programed for, and results for a number of orbits computed on, the IBM 7090 computer. The required variable inputs are α, γ, h_a, and h_p, where h_a is the apogee altitude and h_p is the perigee altitude. The fixed inputs are σ, σ', and R_e. Their respective values, as used in the computations, are 0.00461715 rad, 0.00470245 rad, and 3,441.845 naut miles. The quantities e and a are related to h_a and h_p by

$$e = (h_a - h_p)/(2R_e + h_a + h_p) \quad (13)$$

$$a = [(h_a + h_p)/2] + R_e \quad (14)$$

The average running time to compute both the umbra and penumbra eclipse factors for a given orbit was approximately 0.2 sec.

References

[1] Stoddard, L. G., "Eclipse of artificial earth satellite," Astronaut. Sci. Rev. **III**, 9–16 (April–June 1961).

[2] Pierce, D., "A rapid method for determining the percentage of a circular orbit in the shadow of the earth," Astronaut. Sci. **IX**, 89–92 (Fall 1962).

[3] Patterson, G. B., "Graphical method for prediction of time in sunlight for a circular orbit," ARS J. **31**, 441–442 (1961).

[4] Cunningham, F. G., "Calculation of the eclipse factor for elliptical satellite orbits," NASA TN D-1347 (1962).

[5] Peckham, G. W., "The orbital shadow time of an earth satellite," Institute of Technology, Air Univ., U. S. Air Force, GAE/AE-60-9 (1960).

Exact Kinetic and Approximate Nozzle Recombination Losses

DAVID MIGDAL* AND ARNOLD GOLDFORD†
Grumman Aircraft Engineering Corporation, Bethpage, N. Y.

APPROXIMATE losses due to a nonequilibrium nozzle flow recently have been investigated for space rocket engines and hypersonic ramjets.[1, 2] Although formal methods are available for a multicomponent system,[3, 4] such analyses require extensive computer time. The approximate method of Ref. 1 utilizes Bray's criterion[5] to predict a freezing point where the rate of change of total number of moles required for equilibrium is equal to the recombination rate. This procedure appears to compare well with the exact analyses of Refs. 3 and 4 and some experimental data.[6]

In the approximate method,[1] the equilibrium rate of change is computed as follows:

$$Q = V\frac{d(\Sigma n_i)}{d(A/A^*)}\frac{d(A/A^*)}{dl}$$

Received December 30, 1963; revision received March 16, 1964.

* Senior Gas Dynamics Engineer. Member AIAA.
† Senior Propulsion Engineer. Member AIAA.

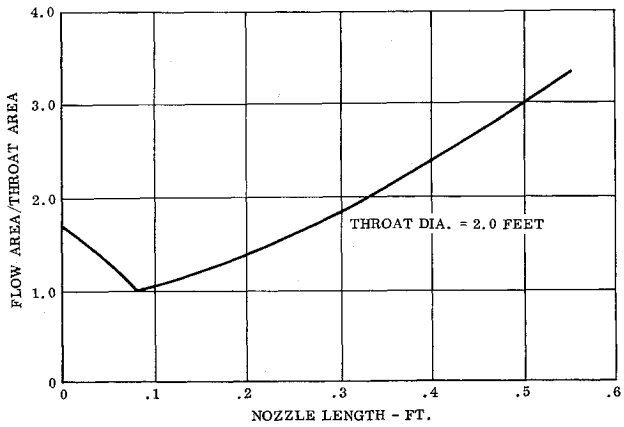

Fig. 1 Nozzle area ratio distribution.

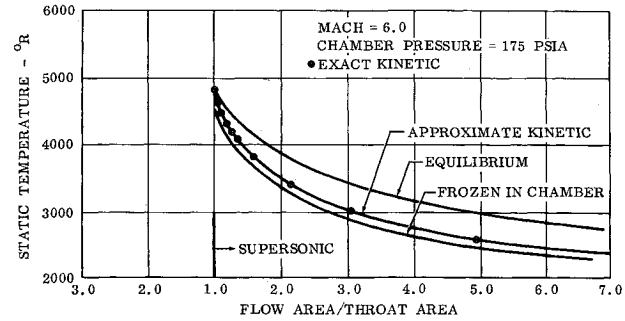

Fig. 2 Comparison of exact and approximate results of static temperature variation with area ratio.

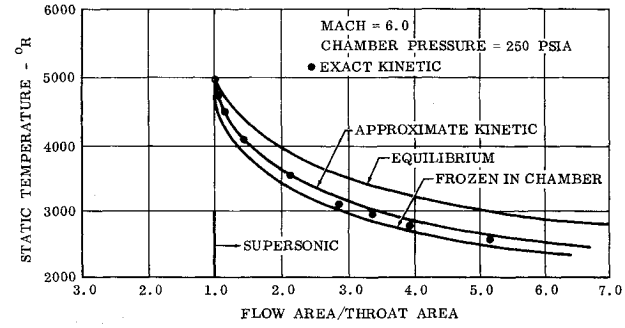

Fig. 3 Comparison of exact and approximate results of static temperature variation with area ratio.

where V is the velocity, n_i the moles of species, A/A^* the nozzle area ratio, and l is the nozzle length. Because of the singularity at the throat, $d(A/A^*) = 0$, we find that freezing is always predicted in the throat region if Q is compared to the recombination rate in this region. To avoid the singularity, equilibrium data were used on either side of the throat and a smooth line faired through the throat region. As a check on the validity of this method, several cases were compared with the more exact analysis of Ref. 7.

The procedure, rate data, and reactions of Ref. 1 were utilized. All of the chamber conditions assumed for comparison of exact and approximate methods are different than those of Ref. 1. Higher enthalpies, representing Mach 6.0 and 8.0 flight in the isotherm and chamber pressures of 175 and 250 psia, were assumed. Stoichiometric hydrogen-air mixture ratios were used in all cases.

The nozzle area distribution vs length is shown in Fig. 1. Figures 2–5 contain the results of the analytically predicted temperature distribution for equilibrium flow, flow frozen at the chamber, exact kinetic flow, and approximate kinetic flow. In Figs. 2 and 3, the flow is frozen at the throat, and the agreement between exact and approximate methods is excellent. This indicated that fairing through the cusped

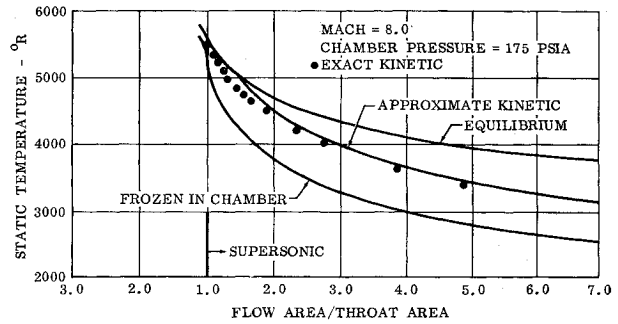

Fig. 4 Comparison of exact and approximate results of static temperature variation with area ratio.

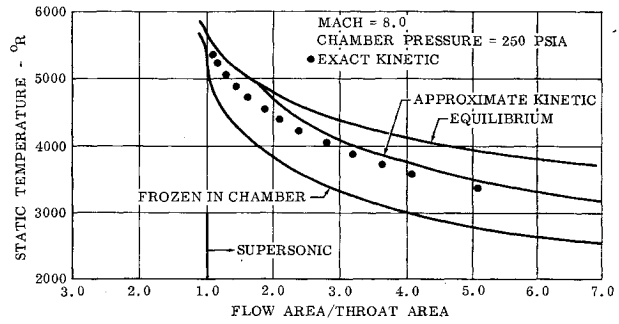

Fig. 5 Comparison of exact and approximate results of static temperature variation with area ratio.

region at the throat does not inadvertently delay an actual throat freezing point. Equilibrium data within 5% of the throat pressure were used in obtaining Q.

In Figs. 4 and 5 the freezing points occur at increasing supersonic area ratio. For these cases, the transition region between near-equilibrium flow and near-frozen flow is longer, and, as expected, the approximate temperature distribution is initially higher than the kinetic values. However, downstream of the transition region the temperatures (and hence specific impulse) again compare quite favorably. It should be noted that the approximate results with the inclusion of data very near the throat do not compare favorably with the more exact kinetic results.

The foregoing results, in conjunction with those presented in Ref. 1, indicate that the approximate method may be sufficiently accurate for engineering estimates. In those cases where the approximate method differs most, that is, with freezing points successively downstream of the throat, the differences between equilibrium and kinetic values of specific impulse are diminishing.

References

[1] Franciscus, L. C. and Lezberg, E. A., "Effects of nozzle recombination on hypersonic ramjet performance: II. Analytical investigation," AIAA J. 9, 2077–2083 (1963).

[2] Simkin, D. J. and Koppang, R. R., "Recombination losses in rocket nozzles with storable propellants," AIAA J. 9, 2150–2152 (1963).

[3] Westenberg, A. A. and Favin, S., "Complex chemical kinetics in supersonic nozzle flow," *Ninth Symposium (International) on Combustion* (Academic Press Inc., New York, 1963), pp. 785–798.

[4] Sarli, V. J. and Blackman, A. W., "Investigation of nonequilibrium flow effects in high expansion nozzles," United Aircraft Corp., B910056-12 (September 1963).

[5] Bray, K. N. C., "Atomic recombination in a hypersonic wind tunnel nozzle," J. Fluid Mech. 6, 1–32 (1959).

[6] Lezberg, E. A. and Franciscus, L. C., "Effects of nozzle recombination on hypersonic ramjet performance: I. Experimental measurements," AIAA J. 9, 2071–2076 (1963).

[7] Zupnik, T. and Nilson, E. N., "One-dimensional finite rate analysis program," Pratt & Whitney Aircraft, Conn., under NASA Contract NASA-366, private communication (November 1963).